tvst

https://doi.org/10.1167/tvst.8.3.7

Article

Biomarkers of Peripheral Nonperfusion in Retinal Venous Occlusions Using Optical Coherence Tomography Angiography

Diogo Cabral[1,2,3], Florence Coscas[1,4], Agnes Glacet-Bernard[4], Telmo Pereira[2], Carlos Geraldes[2,5], Francisco Cachado[2], Ana Papoila[2,5], Gabriel Coscas[1,4], and Eric Souied[4]

[1] Centre Ophtalmologique de l'Odéon, 113 bd Saint Germain, Paris, France
[2] NOVA Medical School I Faculdade de Ciências Médicas, Universidade NOVA de Lisboa, Lisboa, Portugal
[3] Instituto de Oftalmologia Dr. Gama Pinto, Lisboa, Portugal
[4] Department of Ophthalmology, Centre Hospitalier Intercommunal de Creteil, University Paris-Est Creteil, Créteil, France
[5] Centro de Estatística e Aplicações da Universidade de Lisboa, Portugal

Correspondence: Florence Coscas, University Paris-Est Creteil, Ophthalmology, 40 Avenue de Verdun, Creteil, 94000, France. e-mail: coscas.f@gmail.com

Received: 5 November 2018
Accepted: 6 February 2019
Published: 2 May 2019

Keywords: retinal venous occlusion; fractal dimension analysis; lacunarity; optical coherence tomography angiography; fluorescein angiography

Citation: Cabral D, Coscas F, Glacet-Bernard A, Pereira T, Geraldes C, Cachado F, Papoila A, Coscas G, Souied E. Biomarkers of peripheral nonperfusion in retinal venous occlusions using optical coherence tomography angiography. Trans Vis Sci Tech. 2019;8(3):7, https://doi.org/10.1167/tvst.8.3.7

Purpose: To study the association between the assessment of central macular vascular layers by optical coherence tomography angiography (OCT-A) and peripheral nonperfusion evaluated by fluorescein angiography (FA) in patients with retinal venous occlusion (RVO).

Methods: Retrospective review of RVO patients without macular edema. Patients underwent a comprehensive ophthalmic examination including FA, spectral-domain OCT, and OCT-A. Significant ischemia was defined as nonperfusion areas superior or equal to the equivalent of one retinal quadrant on FA. Vascular density (VD) and foveal avascular zone were measured using AngioAnalytics software. Fractal dimension (FD) and lacunarity (LAC) were computed using an algorithm designed by MATLAB (MathWorks, Natick, MA). These variables were used to build a model that translates their association with OCT-A parameters.

Results: There were 48 eyes (48 patients) of which 19 had significant peripheral nonperfusion. Deep capillary plexus FD, VD, and LAC were associated with significant ischemia. In fact, regarding the association with this outcome, LAC alone had the highest area under the curve (AUC = 0.88) followed by FD (AUC = 0.85) and VD (AUC = 0.73). The multivariable model that included LAC and VD, adjusted by best-corrected visual acuity (BCVA) achieved the best performance for the identification of severe nonperfusion on wide-field FA (AUC = 0.93).

Conclusions: The characteristics of the central macular deep capillary plexus on OCT-A may be associated with peripheral nonperfusion on FA, particularly the combination of LAC and vessel density after adjusting by BCVA.

Translational Relevance: Fractal-based metrics applied to OCT-A may become a valuable marker of ischemia in RVO and help guide the clinical decision to perform invasive angiography.

Introduction

Retinal venous occlusion (RVO) is the second most common retinal vascular disorder after diabetic retinopathy and affects approximately 16 million people worlwide.[1] The prognosis and visual outcome is dependent on the amount of retinal ischemia and the presence or absence of macular edema.[2–4]

Until recently, fluorescein angiography (FA) was the only method available to evaluate retinal vascular circulation in RVO; previous studies have shown significant changes in the mean perifoveal intercapillary area, size of the foveal avascular zone (FAZ) and capillary blood flow.[5,6] Optical coherence tomography

angiography (OCT-A) is a simple and noninvasive method for imaging retinal capillaries without injection of contrast dyes. Several studies have explored OCT-A imaging in subjects with RVOs and demonstrated impaired vascular perfusion in both the superficial and deep capillary plexuses (DCPs), FAZ enlargement, intraretinal edema, and microvascular abnormalities.[7–9] Some of these studies have demonstrated an association between capillary network disruption in the DCP and retinal peripheral ischemia.[7] However, the use of qualitative OCT-A criteria for routine evaluation of microvascular abnormalities is limited in scope as it implies a subjective approach.[7] Therefore, recent works have evaluated OCT-A quantitative biomarkers to assess microvascular modifications, but the association between quantitative biomarkers and peripheral ischemia remains to be established. The most widely available metric is vessel density. However, this analysis is little informative of vascular complexity as it only reflects the percentage of the sample area occupied by vessel lumens.[11] On the other hand, fractal-based methods are mathematical approaches that enable us to quantify the visual texture of a branching vascular system. Fractal dimension (FD) and lacunarity (LAC) are two fractal-based parameters that can be seen as counterparts. FD refers to vascular complexity and it is a measure of *how much* space is filled, for example, a FD of 0 reflects an empty square, a FD of 1 reflects a linear structure, and a FD of 2 reflects a filled square. LAC refers to heterogeneity and it is a measure of *how* the branching vessels fill the space: normal capillary networks are homogeneous and score lower values; disrupted capillary networks are heterogeneous and score higher values.[12–14] For instance, low values of FD and higher values of LAC would be obtained in the DCP of eyes with an ischemic RVO.

Presently, there is growing interest in the quantitative analysis of the microvascular architecture following the introduction of OCT-A and its ability to perform high resolution imaging of the retinal microvasculature. Studies applying FD analysis in retinal microvascular diseases (diabetic retinopathy and RVO) have demonstrated significant changes even early in the disease process.[15–17] In RVO, reproducible and reliable quantitative analysis of the microvasculature would be very helpful for evaluating disease severity, progression, and response to treatment.

The aim of this study was to investigate the association between quantitative OCT-A parameters in the capillary plexuses and the angiographic assessment of peripheral ischemia in RVO patients.

Methods

Design and Setting

Retrospective study of consecutive patients diagnosed with retinal vein occlusion, observed at the University Eye Clinic of Creteil between 2015 and 2017 and that followed a *pro re nata* regimen with anti-vascular endothelial growth factor (VEGF) or corticosteroid for macular edema in RVO.

This study was conducted in accordance with the tenets of the Declaration of Helsinki (1964) and French legislation and after approval by the University Paris Est ethical committee. All enrolled patients gave their written informed consent at the time of recruitment.

Participants

Patients were included in the study if they met all the following inclusion criteria: diagnosis of RVO using conventional multimodal imaging (FA and spectral-domain OCT [SD-OCT]). We only included eyes with no evidence of macular edema on SD-OCT to minimize the confounding effect of macular edema on segmentation. Therefore, all subjects received at least three intravitreal anti-VEGF injections prior to the OCT-A evaluation and had then no evidence of macular edema as demonstrated by SD-OCT. The exclusion criteria were diabetic retinopathy, previous retinal surgery, pathologic myopia, epiretinal membrane, or ocular trauma. Patients with poor quality images on OCT-A (signal strength index [SSI] lower than 50) owing to eye movements or media opacities were excluded from this study.

Data Sources

All patients had undergone a comprehensive ophthalmologic examination including best-corrected visual acuity (BCVA) using an Early Treatment Diabetic Retinopathy Study (ETDRS) chart, biomicroscopy, FA, and SD-OCT, as well as SD-OCT angiography, which involved the 3×3 mm area (10°) of the central macula. We used the 3×3 mm acquisition as it provides better axial resolution than larger scans to evaluate capillary morphology.

Image Acquisition and Analysis

Enhanced Depth Imaging (EDI) SD-OCT with automated volume mode of 49 B-scans and macular 30° centered on the fovea was performed with the Spectralis OCT equipment (Heidelberg Engineering,

Inc., Heidelberg, Germany). Retinal structures were evaluated using SD-OCT images.

FA was performed using a 55° lens, and eight peripheral fields were taken just after the filling of all the retinal vessels (between 30 seconds and 90 seconds for most examinations) to evaluate peripheral nonperfusion. An experienced clinician (AGB) graded peripheral nonperfusion on FA from one to six, masked to the corresponding OCT-A images to prevent bias. The grades were as follows: 1–well perfused peripheral retina; 2–questionable nonperfusion because of staining and leakage of dye from the vessel wall in the peripheral retina or because of retinal hemorrhages; 3–presence of moderate nonperfused peripheral area of less than the equivalent of one quadrant; 4–presence of marked nonperfused peripheral area larger than grade 3 and less than two quadrants; 5–presence of severe nonperfused peripheral area larger than grade 4 and less than four quadrants; and finally grade 6–total retinal ischemia including the posterior pole.[18,19]

BCVA was converted to the logarithm of the minimal angle of resolution (logMAR) for statistical evaluation. The OCT-A used in this study (AngioVue; Optovue, Inc.) analyzed the OCT images by using SSADA. A 3×3 mm area, centered on the fovea, was scanned for all the enrolled patients. The device performs each acquisition at a speed of 100 kHz, 70,000 A-scans per second, using a 840-nm superluminescent diode and with a bandwidth of 45 nm; 320 A-scans made up a B-scan while 320 horizontal and vertical lines separated by 9 mm each were sampled in the scanning area in order to form a three-dimensional data cube. Volumetric raster scans were obtained from two horizontal fast transverse scans and two vertical fast transverse scans, both acquired in 3.4 seconds each. The calculated amplitude decorrelation signal from the consecutive B-scans enabled blood flow, and therefore the capillary network, to be clearly visualized. Image analysis was performed by automated retinal segmentation derived from the machine software. In normal subjects, the superficial capillary plexus (SCP) can be seen by using a section starting from the internal limiting membrane (ILM) and selecting sufficient thickness to include the ganglion cell layer, while the two components of the deep plexus (DCP), which bracket the inner nuclear layer (INL), are included in the section defined by the inner border of the INL and the middle of the outer plexiform layer. Images of both SCP and DCP were exported as Tagged Image File Format (TIFF) for quantitative analysis.

Quantitative Variables

Central macula capillary network was evaluated on two steps. First, we used the Angio Analytics software to calculate the relative density of flow as a percentage of the total area. This software has inbuilt a projection artifact removal algorithm that enables us to minimize projection artifacts in the deeper retinal layers.[20] It calculates vessel density by extracting a binary image of the vessels from the gray scale OCT-A en-face image, and then by computing the percentage of pixels of vessels. In this study, we used the whole en face vessel density of both SCP and DCP images. We also analyzed the no-flow areas, using the automated measurement of nonflow, which include the foveal avascular area of the FAZ.

Second, organizational biomarkers were computed on raw images using a custom graphical user interface built in MATLAB (v. r2018a) coding language. Images were binarized using Otsu local threshold method[21] (rolling ball of 15 pixels) and skeletonized using MATLAB custom algorithm. The algorithm using the box counting method at multiple origins divided a skeletonized image into square boxes of equal sizes to estimate FD[12,22] and LAC,[23,24] which are global indices of morphological complexity and structural nonuniformity, respectively.[23] Using OC-TA data, Koulisis et al.[17] have shown an association between FD and RVO severity. The ability of LAC to distinguish homogeneous from heterogeneous branching vascular systems was employed previously in retinal fundus photos. Landini et al.[13] demonstrated that LAC could discriminate eyes with a RVO from normal eyes (RVO eyes presenting with higher LAC values). Popovic et al.[25] demonstrated that LAC could distinguish branching patterns with distinct homogeneity but with similar FD values.

To calculate FD the number of boxes containing a vessel segment were counted and this process was repeated several times with boxes that followed a linear progression of sizes and with different growing directions until a box of half image pixel size was reached. The output value of FD is determined by the slope of the linear regression between $\log(N)$ (where N represents the number of boxes containing the vessel) and $\log(\varepsilon)$ (where ε represents the size of the boxes divided by the size of the image). By plotting the relation above explained as in Figures 1 and 2 (third line, middle), we observed a power-law distribution, FD:

$$\mathrm{FD} = -\frac{\log(N)}{\log(\varepsilon)}.$$

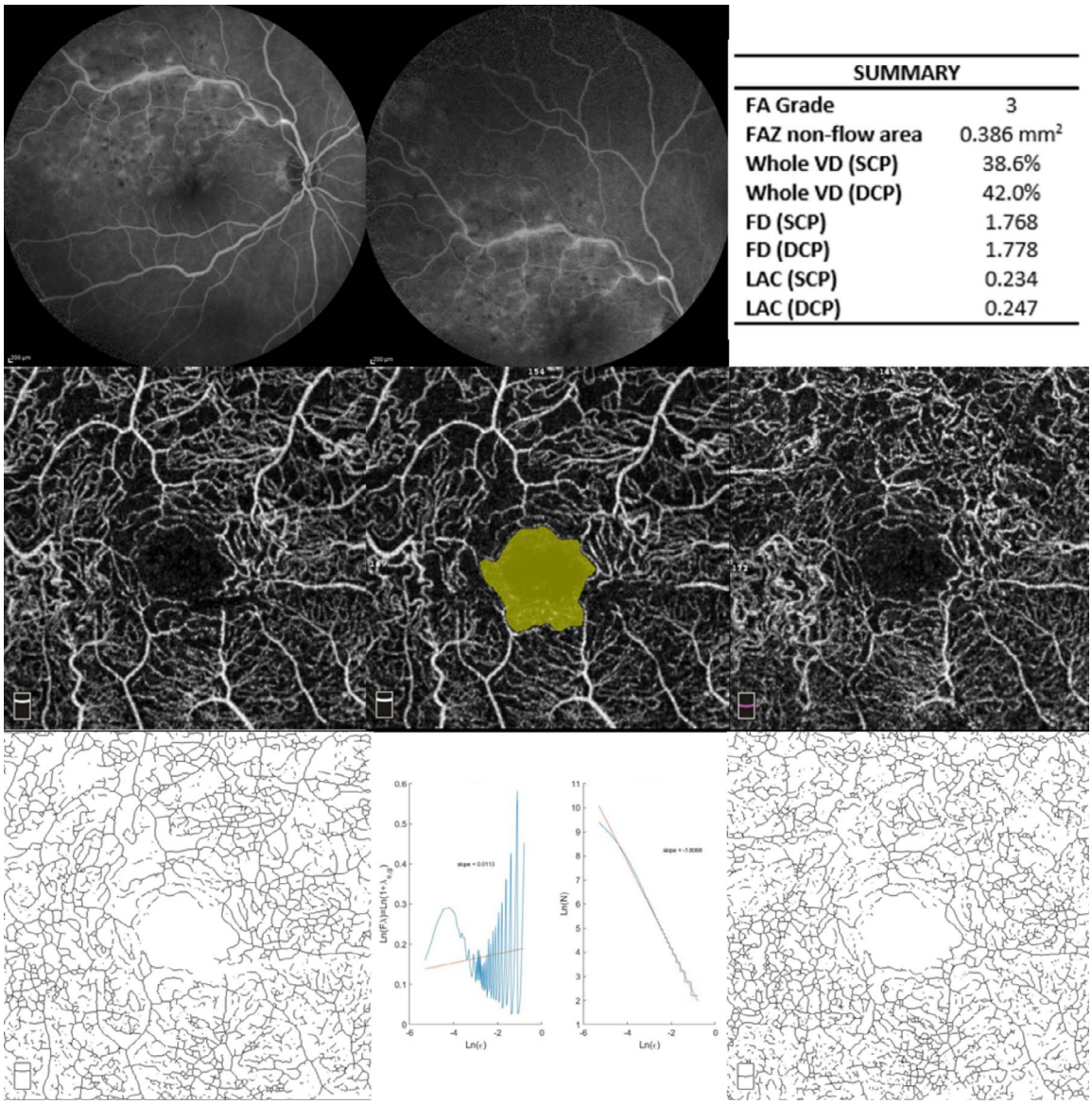

Figure 1. Multimodal imaging in a 68-year-old patient with BRVO (BCVA: 20/25). FA (*first line, right and middle*) shows macular perfusion abnormalities and nonperfusion areas on the supero-temporal quadrant (grade 3). On OCTA, at the SCP (*second line, left*), a few capillary dropouts are seen in the superior sector. Whole en face VD in the SCP was 38.60%. In the DCP (*second line, right*) a few hypoperfused areas are seen. Whole en face VD in the DCP was 42.0%. Superficial nonflow area was 0.386 mm^2 (*second line, middle*). Skeletonization of OCTA images was performed (*third line, left and right*) and box counting analysis performed accordingly (*third line, middle*). Results are summarized on the table (*first line, right*).

The FD varies with the distribution of skeletonized vessels of the image and has a value between 0 and 2. The more complex the pattern, the higher the measured value.

LAC (λ) calculation comes from the variation in pixel density at different box sizes in fixed scans and sliding scans. This value is calculated following a mathematical formula described elsewhere,[24] where σ is the standard deviation (SD) and μ is the mean for pixels per box at this size (ε) at a specific box orientation (g):

$$\lambda_{\varepsilon,g} = \left(\frac{\sigma}{\mu}\right)^2_{\varepsilon,g}.$$

In Figures 1 and 2 (third line, middle), we observed the relation between the Ln(Fλ), the logarithmic value of $\lambda_{\varepsilon,g} + 1$, and log($\varepsilon$), the logarithmic value of the size

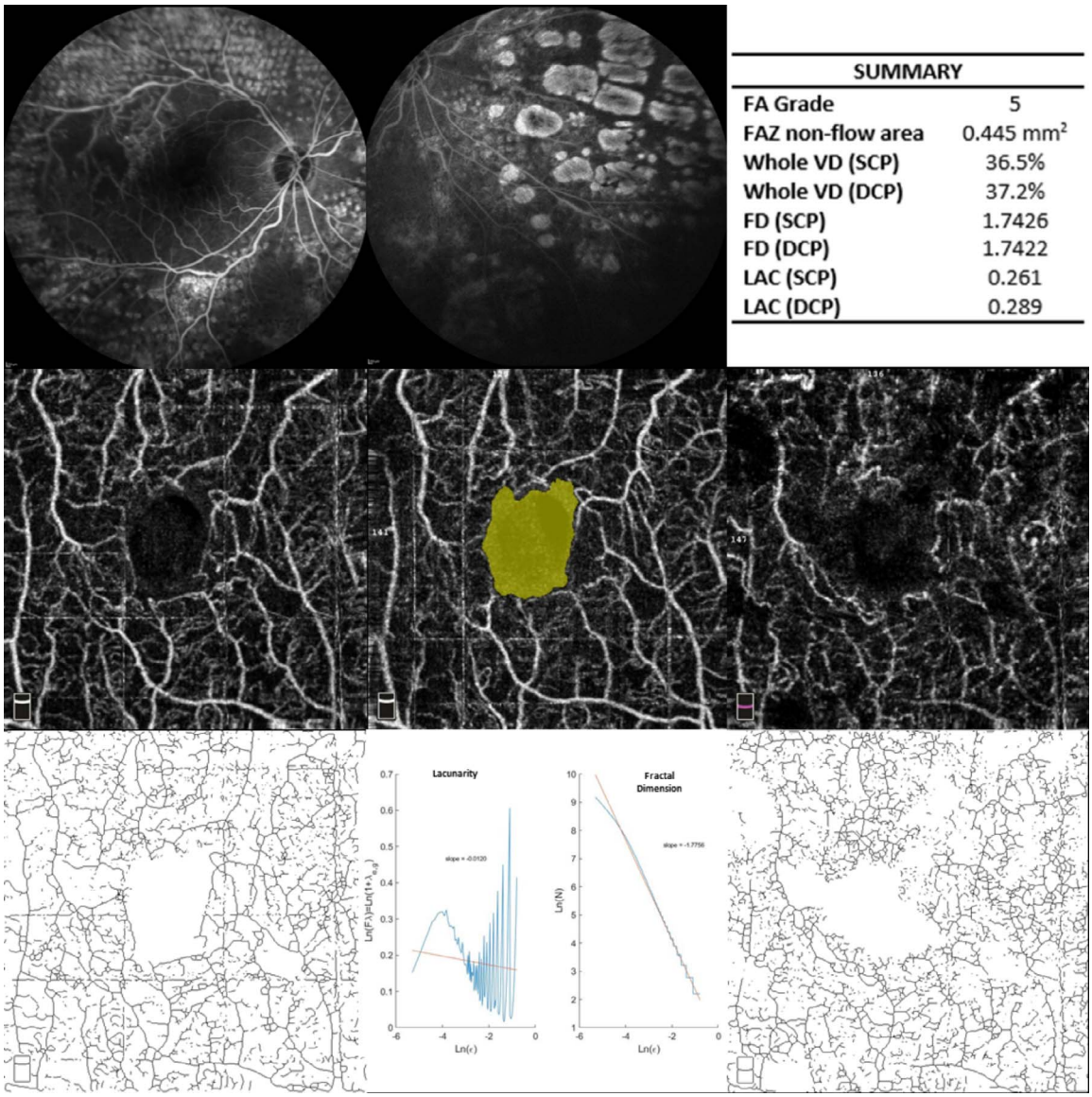

Figure 2. Multimodal imaging in an 81-year-old patient with CRVO (BCVA: 20/40). FA (*first line*) shows macular perfusion abnormalities and severe nonperfused peripheral area (grade 5) and retinal photocoagulation LASER scars. On OCTA, at the SCP (*second line, left*), we observe sparse capillary dropouts. Whole en face VD in the SCP was 38.60%. In the DCP (*second line, right*) sparse hypo perfused areas are seen. Whole en face VD in the DCP was 42.0%. Superficial nonflow area was 0.386 mm^2 (*second line, middle*). Skeletonization of OCTA images was performed (*third line, left and right*) and box counting analysis performed accordingly (*third line, middle*). Results are summarized on table (*first line, right*). CRVO, central RVO.

of the boxes divided by the size of the image. To obtain the mean LAC $\bar{\lambda}_g$ for orientation g, the following formula was used:

$$\bar{\lambda}_g = \frac{\sum \lambda_{\varepsilon,g}}{\text{Number of Boxes}}.$$

To calculate the mean lacunarity of an image pattern (LAC) and have a more precise value, the algorithm runs the box counting method in K different grid orientations, which leads to the following formula:

$$\text{LAC} = \left(\sum [\bar{\lambda}_g]\right)/\text{K}.$$

LAC varies with both gaps and heterogeneity of skeletonized vessels and has a value superior to 0, which means a completely homogeneous image. The more heterogeneous the pattern, the higher the measured value. FD and LAC results were automat-

ically exported into a comma separated file for further analysis.

Statistical Analysis

We performed an exploratory analysis of the demographic, clinical, FA (peripheral nonperfusion areas), and OCT-A (FAZ nonflow area, LAC, vessel density, and FD) measurements. Continuous variables are presented as mean and SD or median and interquartile range (IQR: 25th percentile–75th percentile), as appropriate. We analyzed the association of each of these variables with the anatomic classification of RVO (central RVO [CRVO] versus branch RVO [BRVO]) and with the primary outcome peripheral nonperfusion.

These parameters were further studied using generalized additive models[22] (GAMs) for binary response (ischemic versus nonischemic RVO). Partial functions that represent the referred associations were obtained, and because their functional form has shown to be linear, generalized linear models (GLMs) were then used.

Models' performance regarding the trade-off between their goodness of fit and complexity was measured by the Akaike Information Criterion (AIC), and their discriminative ability to distinguish between ischemic and nonischemic RVO was measured by the area under the receiver operating characteristic (ROC) curve (AUC). Lower values of AIC indicate a better goodness of fit while higher AUC values indicate better discriminative ability.

Considering the group of univariable models (from the capillary plexus analysis) that obtained the best performance, multivariable models were fitted using a baseline model (with ischemic RVO as outcome and with only the covariate vascular density [VD]). Two multivariable models were constructed adding each one of the remaining OCT-A covariates (FD and LAC) at a time. Additionally, the model with the best performance was adjusted by the variable BCVA.

The goal of this analysis was to quantify the added contribution of each of these potential biomarkers to the performance of the baseline model. Accordingly, a DeLong's test was performed to assess the significance of the difference between the baseline and the best multivariable models' AUC. Schematic diagrams of the statistical modeling are available as a supplementary figure (Supplementary Fig. S1). A level of significance $\alpha = 0.05$ was considered. All statistical analyses were performed using R.[26]

Results

A total of 48 eyes of 48 consecutive RVO patients were included in this study: CRVO (25 eyes, 52.1%), hemicentral RVO (HCRVO; 3 eyes, 6.2%), and BRVO (20 eyes, 41.7%). For statistical purposes, HCRVO and CRVO eyes were analyzed together in the CRVO subgroup.

The age of the patients at presentation ranged from 45.3 to 88.7 years (mean, 68.9; SD, 12.0), and 19 (39.6%) study patients were female. The median visual acuity was 0.40 (IQR: 0.01–0.07) logMAR. On FA, 13 (27.1%) eyes were evaluated as grade 1, 7 (14.6%) eyes as grade 2, 9 (18.8%) eyes as grade 3, 8 (16.7%) eyes as grade 4, 5 (10.4%) eyes as grade 5, and 6 (12.5%) eyes (corresponding to 17.9% of CRVO eyes) as grade 6. The demographic, clinical, and FA characteristics of the study patients have been summarized in Table 1.

Both the SCP and DCP were evaluated using OCT-A. Regarding the quantitative evaluation of the SCP in the CRVO group, the median FAZ area was 0.49 mm^2 (IQR: 0.37–0.61), the mean vessel density was 38.07 (5.04)%, mean FD value was 1.746 (0.037), and median LAC was 0.250 (IQR: 0.234–0.276) while in the BRVO group, the median FAZ area was 0.54 mm^2 (IQR: 0.36–0.80), mean vessel density was 38.68 (5.73)%, FD median value was 1.764 (IQR: 1.747–1.777), and LAC median value was 0.261 (IQR: 0.249–0.295).

Regarding the quantitative evaluation of the DCP in the CRVO group, the mean vessel density was 39.54 (6.67)%, FD median value was 1.768 (IQR: 1.742–1.789), and LAC median was 0.265 (IQR: 0.232–0.290), while in the BRVO group, mean vessel density was 42.770 (7.259)%, FD median value was 1.779 (IQR: 1.754–1.792), and LAC median was 0.249 (IQR: 0.235–0.303). There was no significant difference (all *P*-values were higher than 0.05) between the CRVO and BRVO groups in any of the analyzed parameters. Figures 1 and 2 show the OCT images of two representative study patients. Results of the differences between the ischemic and non-ischemic RVO groups are presented in Table 2.

As can be seen in Table 3, the DCP variables obtained the best performances; thus, we analyzed the performance of the models studying the association of the quantitative DCP variables with significant peripheral nonperfusion, defined as FA nonperfusion areas $\geq$ one retinal quadrant. The variables LAC (AUC = 0.88; 95% confidence interval [CI]: 0.755–0.998; AIC = 37.02) and VD (AUC = 0.73; 95% CI:

Table 1. Demographic and Clinical Data of Patients With RVO

	Total Group ($n = 48$)	Subgroup 1 (CRVO and HCRVO), $n = 28$	Subgroup 2 (BRVO), $n = 20$
Age, y	68.9 (12.0)	69.09 (12.31)	68.63 (11.80)
Female, *n* (%)	19 (39.6)	10 (35.7)	9 (45.0)
BCVA (logMAR)	0.40 (0.01–0.70)	0.35 (0.01–0.60)	0.45 (0.01–0.70)
Nonperfusion grade on FA, *n* (%):			
1 (absent)	13 (27.1)	9 (32.1)	4 (20.0)
2 (questionable)	7 (14.6)	4 (14.3)	3 (15.0)
3 (<1 quadrant)	9 (18.8)	4 (14.3)	5 (25.0)
4 (<2 quadrants)	8 (16.7)	2 (7.1)	6 (30.0)
5 (<4 quadrants)	6 (12.5)	4 (14.3)	2 (10)
6 (all retina)	5 (10.4)	5 (17.9)	—

Continuous variables were presented as mean and SD or median and IQR (25th percentile–75th percentile), as appropriate.

0.570–0.892; AIC = 53.1) achieved the best and the worst results, respectively. In the multivariable models, the two remaining OCT-A parameters were added to VD as this parameter is the one most widely available in the commercial software and so, extensively studied. Delong's test results revealed that the model including VD and LAC, after adjusting for BCVA (referred to as the VD+LAC+BCVA model in Table 3) led to a statistically significant increase in the discriminative ability ($P = 0.02$) from model with VD alone.

Discussion

Using conventional OCT-A parameters and fractal-based potential biomarkers, we identified vascular patterns in the central macula associated with peripheral nonperfusion on FA and also observed evidence for the modification of the DCP in RVO. Further, considering the three analyzed assessment criteria, the model combining LAC and vessel density achieved the best performance in associating the

Table 2. Patients' Characteristics, OCT-A Parameters (Explanatory Variables) and Univariable Analysis for the Outcome Significant Ischemia

	Peripheral Nonperfusion < 1Q ($n = 22$)	Peripheral Nonperfusion >1Q ($n = 19$)	*P* Value
Demographic and clinical characteristics			
Age	68.78 (11.28)	68.84 (13.30)	0.988
Sex (female), *n* (%)	10 (45.5)	6 (31.6)	0.366
BCVA	0.32 (0.01–0.50)	0.70 (0.3–1.3)	0.028
SCP parameters			
FAZ nonflow area (mm^2)	0.56 (0.32)	0.78 (0.62)	0.179
VD (%)	39.71 (5.92)	36.46 (4.37)	0.065
FD	1.759 (0.033)	1.727 (0.077)	0.142
LAC	0.24 (0.06)	0.28 (0.10)	0.171
DCP parameters			
VD (%)	43.05 (6.87)	37.35 (6.10)	0.016
FD	1.781 (0.019)	1.722 (0.022)	0.005
LAC	0.243 (0.023)	0.338 (0.090)	0.004

Continuous variables were presented as mean and SD or median and IQR (25th percentile–75th percentile), as appropriate. VD, whole en face vessel density.

Table 3. Models' Performance Analysis Using Superficial and DCP Parameters (Explanatory Variables) for Discriminating Eyes With Significant Ischemia (Outcome Variable)

Univariable Models	AUC (95% CI)	AIC
SCP		
FAZ nonflow area	0.61 (0.43–0.79)	58.23
VD	0.66 (0.49–0.83)	56.73
FD	0.71 (0.55–0.88)	55.45
LAC	0.74 (0.59–0.90)	56.22
DCP		
VD	0.73 (0.57–0.89)	53.11
FD	0.85 (0.73–0.97)	42.25
LAC	0.88 (0.76–1.0)	37.07
Clinical characteristics		
BCVA	0.71 (0.55–0.87)	54.49
Multivariable models		
VD + FD	0.86 (0.75–0.98)	43.47
VD + LAC	0.89 (0.78–1.00)	37.69
VD + LAC + BCVA	0.93 (0.85–1.00)	36.30

VD, whole en face vessel density.

quantitative OCT parameters with peripheral nonperfusion on FA.

Although previous qualitative studies of the central macular vasculature in RVO have provided important insights,[7,8,17] our results suggest that we should also consider several quantitative parameters. We present additional insights into the modifications of the DCP based on our results and other previous studies. In contrast to other short-term OCT-A studies, our report is the first involving both LAC and FD to characterize the organization of the vascular plexus.

The technological progress in OCT-A has enabled us to study in detail the capillary abnormalities induced by veno-occlusive disease. Various publications support the view that the DCP is more modified than the SCP in RVO, possibly reflecting its relative watershed location between the retinal vascular and choroidal circulations that makes it prone to ischemic alterations. Consequently, the association between these changes and the clinical features of RVO have been thoroughly studied.[7,8,27–29]

Areas of retinal nonperfusion are commonly assessed by FA.[4] However, because FA is not usually repeated, routine ischemic changes are often inferred by the presence of indirect features such as neovascularization, macular edema, or changes in vision.[29] Coscas et al.[7] found that perifoveal capillary arcade changes in the SCP and network disruption in the DCP were significantly correlated with peripheral nonperfusion (10-disc diameters or more on FA). However, the association between perifoveal capillary disruption and peripheral nonperfusion on FA was only noted in 63% of eyes, and the intra- and interobserver agreement for OCT-A parameters varied between 0.61 and 0.82.[7] Using automated quantitative analysis, we have corroborated these findings consistently showing an association between DCP organizational metrics (FD and LAC) and significant peripheral nonperfusion on FA (defined as at least 10 disc diameters).

VD is a readily available and well-studied OCT-A parameter. Recently, Seknazi et al.[27] demonstrated a significant correlation between automatically quantified central macula (3×3 mm) VD (less than 46%) on OCT-A and peripheral nonperfusion on FA. The authors concluded that central macula changes on OCT-A could help identify high-risk retinal vein occlusion patients who may benefit from further evaluation using FA. However, vessel density, as a potential biomarker, lacks the informative power to characterize distinct patterns. This deficiency was reflected in a large dispersion of values and, therefore, the authors could not identify a clear threshold for macular VD beyond which retinal nonperfusion was always present.[27] Our results confirm that DCP vessel density has a linear association with significant peripheral nonperfusion (P-value = 0.023). Even so, this potential biomarker alone had the worst model performance among the three assessed criteria. Nevertheless, the performance of this quantitative parameter may be improved if VD is modeled together with LAC or FD.

LAC is a measure of vascular nonuniformity using a box counting method. The values are calculated through mathematical formulae using pixel distribution, where higher values reflect heterogeneity and lower values reflect an homogenous vascular structure.[23] As previously observed by OCT-A imaging, the microvascular features of the DCP are modified in RVO patients by capillary abnormalities and areas of absent deep vascular plexus flow.[7,8] This qualitative observation translates into higher LAC within the DCP, irrespective of the presence of cystoid macular edema (CME).[8] Following this observation, one would expect a DCP pattern with irregular nonperfusion areas and abnormal capillaries (higher LAC) to be associated with more nonperfusion areas on FA (ischemic RVO). Our results showed a linear and positive association between LAC and peripheral

nonperfusion, consistent with the above expectation. Moreover, our analysis demonstrated that LAC and BCVA improved the discriminative performance of a model containing VD alone. These findings emphasize, for the first time, LAC as a novel parameter for image analysis of the DCP.

FD analysis quantifies the variations in space filling using the box-counting method and provides a way of characterizing an object in terms of complexity described as "fractal dimension" (FD). The box counting method divides a skeletonized image into square boxes of equal sizes and counts the number of boxes containing a vessel segment. In two dimensional images, the FD has a value between 0 and 2 with higher values indicating increased pattern complexity.[30] Koulisis et al.[17] quantitatively evaluated the central macular microvasculature in human subjects with RVO, using OCT-A, and found a statistically significant difference in FD of all the vascular layers in subjects with BRVO and CRVO compared with controls and unaffected fellow eyes. Also, FD progressively decreased as the clinical severity of RVO increased (BRVO versus CRVO). The authors suggested that OCT-A-based metrics of morphology and density could be useful in quantifying RVO severity.[17] Our results showed no significant differences between the BRVO and CRVO groups in FD and LAC. However, the clinical characteristics were not statistically different between these groups in our study possibly due to the inclusion of eyes without CME. This suggests that an anatomic binary classification (BRVO versus CRVO) for RVO severity lacks direct correspondence with morphological changes and that an objective and quantitative classification system would be very useful in clinical trials and clinical management.

Based on the current study, as well as previous anatomic and clinical studies, we propose that quantitative measurements of the central macular DCP are a potentially useful biomarker of disease severity in RVO. This is noteworthy since the parameters are derived from a 3×3 mm macular scan obtained from noninvasive technology. In the future, OCT-A based scores of the central macula may help guide the clinical decision to perform invasive angiography.

The strengths of our study include the use of an automatic image analysis protocol and the use of global indices of morphological complexity and structural nonuniformity. We included only patients without CME after therapy for RVO complications, overcoming a limitation of previous studies where it was not clear how the segmentation variability due to macular edema was addressed.[29] Moreover, our results were obtained with a commercially available device and not with a prototype, overcoming another limitation of previous OCT-A studies. Modifications in the DCP accessed by OCTA must be interpreted with caution. Data that are obtained following processing of OCTA images (binarization and skeletonization) are subject to several artifacts (e.g., vitreous opacities, cataracts, or other media opacities) including vessel projection artifacts from the SCP, which could impact the results. A strength of this study is that we have used a SD-OCTA software that has inbuilt the algorithm developed by Zhang et al.[20] to minimize projection artifacts in the DCP. Our current analyses indicate that the magnitude of DCP modifications is most notable in the most ischemic cases of RVO, which is consistent with most of the qualitative studies on this field.[7,27]

Our study limitations include a small sample size, inclusion of patients previously treated for macular edema, and technical limitations that are inherent in the current technology. Future works may investigate our hypothesis before macular edema supervenes.

Also, we must be aware of the limitations of interpreting the vascular plexus, a three-dimensional structure, using a two-dimensional approach.

In conclusion, we have demonstrated the feasibility of using OCT-A for objective quantitation of RVO severity. With the increasing availability of this technology, evaluation of OCT-A metrics may become a valuable tool to help guide the clinical decision to perform invasive angiography. Meanwhile, we recommend larger, prospective, and longitudinal studies to evaluate the organization of retinal capillaries with box counting methods over the course of treatment for RVO complications.

Acknowledgments

Disclosure: **D. Cabral**, None; **F. Coscas**, None; **A. Glacet-Bernard**, None; **T. Pereira**, None; **C. Geraldes**, None; **F. Cachado**, None; **A. Papoila**, None; **G. Coscas**, None; **E. Souied**, None

References

1. Rogers S, McIntosh RL, Cheung N, et al. The prevalence of retinal vein occlusion: pooled data

from population studies from the United States, Europe, Asia, and Australia. *Ophthalmology*. 2010;117:313–319.e1.
2. Campochiaro PA, Brown DM, Awh CC, et al. Sustained benefits from ranibizumab for macular edema following central retinal vein occlusion: twelve-month outcomes of a phase III study. *Ophthalmology*. 2011;118:2041–2049.
3. McIntosh RL, Rogers SL, Lim L, et al. Natural history of central retinal vein occlusion: an evidence-based systematic review. *Ophthalmology*. 2010;117:1113–1123.e15.
4. Coscas G, Anat Loewenstein A, Augustin A, et al. Management of retinal vein occlusion – consensus document. *Ophthalmologica*. 2011; 226:4–28.
5. Remky A, Wolf S, Knabben H, Arend O, Reim M. Perifoveal capillary network in patients with acute central retinal vein occlusion. *Ophthalmology*. 1997;104:33–37.
6. Parodi MB, Visintin F, Della Rupe P, Ravalico G. Foveal avascular zone in macular branch retinal vein occlusion. *Int Ophthalmol*. 1995;19: 25–28.
7. Coscas F, Glacet-Bernard A, Miere A, et al. Optical coherence tomography angiography in retinal vein occlusion: evaluation of superficial and deep capillary plexa. *Am J Ophthalmol*. 2016; 161:160–171e2.
8. Spaide RF. Volume-rendered optical coherence tomography of retinal vein occlusion pilot study. *Am J Ophthalmol*. 2016;165:133–144.
9. Rispoli M, Savastano MC, Lumbroso B. Capillary network anomalies in branch retinal vein occlusion on optical coherence tomography angiography. *Retina*. 2015;35:2332–2338.
10. Spaide RF. Volume-rendered angiographic and structural optical coherence tomography. *Retina*. 2015;35:2181–2187.
11. Coscas F, Sellam A, Glacet-Bernard A, et al. Normative data for vascular density in superficial and deep capillary plexuses of healthy adults assessed by optical coherence tomography angiography. *Invest Ophthalmol Vis Sci*. 2016;57: OCT211–OCT223.
12. Masters BR. Fractal analysis of the vascular tree in the human retina. *Annu Rev Biomed Eng*. 2004; 6:427–452.
13. Landini G, Murray PI, Misson GP. Local connected fractal dimensions and lacunarity analyses of 60 degrees fluorescein angiograms. *Invest Ophthalmol Vis Sci*. 1995;36:2749–2755.
14. Tolle CR, McJunkin TR, Gorsich DJ. An efficient implementation of the gliding box lacunarity algorithm. *Phys D Nonlinear Phenom*. 2008;237:306–315.
15. Zahid S, Dolz-Marco R, Freund KB, et al. Fractal dimensional analysis of optical coherence tomography angiography in eyes with diabetic retinopathy. *Invest Opthalmol Vis Sci*. 2016;57: 4940.
16. Anegondi N, Chidambara L, Bhanushali D, Gadde S, Yadav N, Sinha Roy A. An automated framework to quantify areas of regional ischemia in retinal vascular diseases with OCT angiography. *J Biophotonics*. 2017;Jul(12):303–325.
17. Koulisis N, Kim AY, Chu Z, et al. Quantitative microvascular analysis of retinal venous occlusions by spectral domain optical coherence tomography angiography. *PLoS One*. 2017; (Vdi):1–14.
18. Glacet-bernard A, Coscas G, Chabanel A, Zourdani A, Samama MM. Prognostic factors for retinal A prospective study of 175 cases. *Ophthalmology*. 1996;(March 1986):551–560.
19. The Central Vein Occlusion Study Group N Report. A Randomized clinical trial of early panretinal photocoagulation for ischemic central vein occlusion. *Ophthalmology*. 1995;102:1434–1444.
20. Zhang M, Hwang TS, Campbell JP, et al. Projection-resolved optical coherence tomographic angiography. *Biomed Opt Express*. 2016; 7:816.
21. Otsu N. A threshold selection method from gray-level histograms. *IEEE Trans Syst Man Cybern*. 1979;9:62–66.
22. Moissy F. Computing a fractal dimension with Matlab: 1D, 2D and 3D Box-counting. 2008. Accessed September 18, 2017.
23. Smith TG, Lange GD, Marks WB. Fractal methods and results in cellular morphology—Dimensions, lacunarity and multifractals. *J Neurosci Methods*. 1996;69:123–136.
24. Karperien A. FracLac for ImageJ. http://rsb.info.nih.gov/ij/plugins/fraclac/FLHelp/Introduction.htm. Accessed September 18, 2017.
25. Popovic N, Radunovic M, Badnjar J, Popovic T. Fractal dimension and lacunarity analysis of retinal microvascular morphology in hypertension and diabetes. *Microvasc Res*. 2018;118:36–43.
26. R Core Team. R: A Language and Environment for Statistical Computing. Vienna, Austria. 2013. Retrieved from http://www.r-project.org/
27. Seknazi D, Coscas F, Sellam A, et al. Optical coherence tomography angiography in retinal vein occlusion. Correlations between macular

vascular density, visual acuity, and peripheral nonperfusion area on fluorescein angiography. *Retina*. 2017:1–9.
28. Kashani AH, Lee SY, Moshfeghi A, Durbin MK, Puliafito CA. Optical coherence tomography angiography of retinal venous occlusion. *Retina*. 2015;35:2323–2331.
29. Kashani AH, Chen C-L, Gahm JK, et al. Optical coherence tomography angiography: a comprehensive review of current methods and clinical applications. *Prog Retin Eye Res*. 2017;60:66–100.
30. Lopes R, Betrouni N. Fractal and multifractal analysis: a review. *Med Image Anal*. 2009;13:634–649.